Journal of Materials Chemistry C

PAPER

Cite this: J. Mater. Chem. C, 2015, 3, 1751

Solvent-tunable PDMS microlens fabricated by femtosecond laser direct writing

Dong-Xiao Lu,[b] Yong-Lai Zhang,*[a] Dong-Dong Han,[a] Huan Wang,[a] Hong Xia,[a] Qi-Dai Chen,[a] Hong Ding[c] and Hong-Bo Sun*[ab]

Received 30th November 2014
Accepted 19th December 2014

DOI: 10.1039/c4tc02737j

www.rsc.org/MaterialsC

Reported here is the fabrication of solvent-tunable polydimethylsiloxane (PDMS) microlenses using the femtosecond laser direct writing (FsLDW) technique. PDMS microlenses with equation-defined profiles, including both spherical microlens and aspheric hyperboloid microlens, have been fabricated according to preprogrammed models. In addition to excellent optical performance derived from the high accuracy and smooth surface, the resultant PDMS microlenses also show unique solvent-tunable properties; the focal length could be dynamically tuned by organic solvents of different solubility parameters. To obtain better control over the tunable property, a PDMS microlens has been flexibly integrated with a microfluidic device. Under the stimulation of different solvents, its tunable imaging performance has been demonstrated in a controlled manner.

Introduction

As important optical components, microlenses have been paid much attention due to their broad applications in the field of micro-optics.[1] For instance, miniaturized microlenses with feature size ranging from hundreds of microns to tens of nanometers have been widely used in optical communication,[2] miniaturized optical systems,[3] laser beam shaping and steering,[4,5] optical sensing, as well as various biomedical imaging applications.[6,7] Over the past few decades, the rapid development of micronanofabrication techniques, represented by classical "top-down" and "bottom-up" approaches, continues to stimulate the progress of microoptics. As representative examples, various microlenses have been readily fabricated through typical techniques including photolithography,[8] dry etching,[9] soft lithography,[10] polymer jet printing,[11] ultraviolet (UV) imprinting,[12] hot embossing[13] and so on.[14] However, in most cases, the above-mentioned techniques do not allow flexible integration of the as-obtained microlens with given devices, such as lab-on-a-chip systems and functional biomedical devices, which significantly limits their potential applications in various miniaturized optical systems. More importantly, the surface profile of a microlens cannot be defined exactly as a mathematical model, for instance, in the case of an aspheric microlens. The profile deformation would significantly affect their optical performance and restrict their applications. As the motivation for designable fabrication and integration of microoptical devices continues to intensify, micro-nanofabrication techniques that are capable of high-precision and three-dimensional (3D) manufacturing have emerged as a promising solution. As an enabler for 3D microstructures, the femtosecond laser direct writing (FsLDW) technique may shed new light on the development of high-performance micro-optical components.[15–17]

In previous works reported by our group[18–22] and others,[23,24] the powerful FsLDW technique has already proved its value in the fabrication of 3D micronanostructures over a wide range of materials.[15] Notably, in the field of microoptics, aspheric microlens arrays with sub-20 nm precision have been successfully fabricated by Wu *et al.*,[25,26] based on the commercial epoxy-based negative photoresist SU-8. Žukauskas *et al.*[27] demonstrated the fabrication of high optical quality conical microlenses and closely packed arrays by FsLDW using a novel hybrid organic–inorganic photoresin, SZ2080. However, the aforementioned methods are generally used for the fabrication of solid-state microlenses with fixed profiles, which do not allow dynamic tuning of their optical performance. With the rapid development of automatic and intelligent optical systems, it is much desired to fabricate dynamically tunable soft microlenses that are suitable for some rigorous applications, such as real-time information acquisition, zooming in/out for imaging and high-definition displays. To this end, mechanical pressure-tunable microlenses that consist of a chamber and a transmutable membrane have been successfully developed using elastic, optically transparent, and low-cost soft materials, for instance, polydimethylsiloxane (PDMS).[28–30] Large tunability of lens optical parameters, such as focal length and even lens type, could be realized by varying the applied liquid or gas pressure.

[a]State Key Laboratory on Integrated Optoelectronics, College of Electronic Science and Engineering, Jilin University, 2699 Qianjin Street, Changchun 130012, China. E-mail: yonglaizhang@jlu.edu.cn; hbsun@jlu.edu.cn

[b]College of Physics, Jilin University, 2699 Qianjin Street, Changchun 130012, China

[c]State Key Laboratory of Inorganic Synthesis and Preparative Chemistry, College of Chemistry, Jilin University, 2699 Qianjin Street, Changchun, 130012, China

Nevertheless, these lenses usually require external controls or power supplies, which make the whole system bulky and complicated.

As an alternative, stimuli-responsive materials that are sensitive to ambient conditions hold great promise for the fabrication of tunable smart microlenses.[31] However, there is still a lack of nanotechniques that permit designable prototyping of these smart materials. Recently, with the help of the FsLDW technique, we successfully fabricated protein (bovine serum albumin, BSA) microlenses that feature rapid and reversible responsive behavior under chemical stimulation.[32] The unique tunability and full biocompatibility make the BSA microlenses promising for various optical, electronic, and biomedical applications. To date, despite the fact that FsLDW techniques have made great contributions to high-performance optical microdevices, continued efforts in programmable fabrication of microoptical components based on more functional materials are still highly required to realize their full potential.

As a typical soft material, PDMS is optically clear, chemically inert, non-toxic, and biologically compatible. It has been widely used in various scientific fields, such as microfluidic devices, flexible and transparent substrates, as well as biomedical applications. However, in most cases, the fabrication of PDMS-based microstructures is limited to the soft lithography technique, which takes advantage of its unusual rheological properties. Despite the fact that PDMS allows direct prototyping through either two-photon microfabrication or laser ablation,[33,34] few attempts have been made at the integration of PDMS-based soft optical components. This has encouraged us to develop solvent-tunable soft microlenses using PDMS as basic material by the FsLDW technique, since PDMS is very sensitive to organic solvents.

In this paper, we report the fabrication and *in situ* integration of PDMS microlenses by the FsLDW technique without the use of any mask or duplicated templates. As a proof-of-concept, spherical microlens and aspheric hyperboloid microlens have been fabricated according to preprogrammed 3D models. Taking advantage of the "3D printing" feature of the FsLDW technique, any microoptical devices could be fabricated and integrated with given devices. Interestingly, the as-fabricated PDMS microlenses show controllable and reversible response to surrounding solvents. By integrating the smart microlenses with microfluidic devices, the focal length could be dynamically tuned under the stimulation of different microfluids. The smart solvent-tunable PDMS microlens may find broad applications in the fields of microoptics and optofluidics. The FsLDW fabrication of PDMS microstructures holds great promise for the development of many advanced microoptical devices such as intelligent robots, detection windows, smart cameras, and biomimetic compound eyes.

Experimental

FsLDW fabrication of PDMS microlenses

Photosensitive PDMS photopolymer was prepared by adding thioxanthen-9-one (5 mg) as photosensitizer to commercial PDMS precursor (5 g) at a mass ratio of 1 : 1000 (w/w). In this work, femtosecond laser pulses (780 nm central wavelength, 80 MHz repetition rate, 120 fs pulse width) were used for the fabrication. In a typical FsLDW run, the laser beam was tightly focused into photosensitive PDMS photopolymers using an oil-immersion objective lens with high numerical aperture (60 ×, NA = 1.4), the immersion oil having a refractive index of 1.514–1.516. Multi-photon absorption-induced photocrosslinking occurs in the central area of the focal spot with a diameter of ~200 nm. The incident laser energy was measured to be 40 mW. The PDMS microlens was directly "written" out by scanning the laser focal point with an exposure time of 1000 μs according to computer designed structures. After FsLDW of the entire lens structure, unpolymerized PDMS photopolymer was removed in ethyl acetate; the soft microlens was thus successfully prepared.

Characterization

The surface morphologies of the microlens samples were characterized by a scanning electron microscope (SEM) operating at 10.0 keV. Atomic force microscopy (AFM) images of the microlens microstructures were obtained from a Digital Instruments NanoScope IIIa in tapping mode. Optical micrographs were obtained with a Motic BA400 microscope and a charge-coupled device.

Results and discussion

The fabrication of a PDMS microlens by FsLDW is schematically illustrated in Fig. 1. In our work, the femtosecond laser pulse with 780 nm central wavelength was tightly focused into photosensitive PDMS photopolymers to trigger photopolymerization through a multi-photon absorption process. Notably, photocrosslinking only occurs in the central area of the focal spot, and in this manner, any desired microstructures could be directly "written" out by scanning the laser focal point according to preprogrammed 3D patterns. After FsLDW of the entire lens structure, unpolymerized PDMS photopolymers

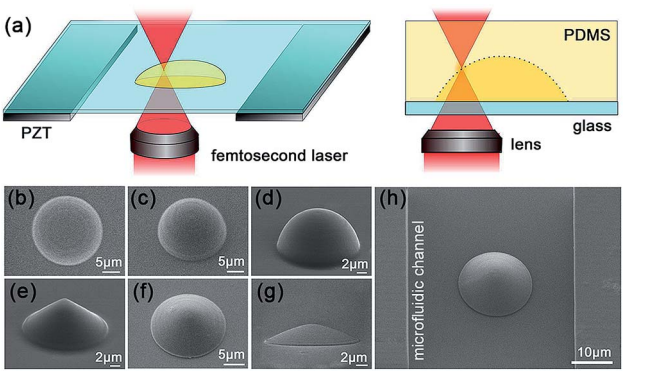

Fig. 1 (a) Schematic illustration of the FsLDW fabrication of a PDMS microlens. The right figure is the side view of the system. (b–d) SEM images of a spherical PDMS microlens from different view angles; (e–g) SEM images of an aspheric hyperboloid microlens from different view angles; (h) SEM image of an aspheric hyperboloid microlens integrated within a microfluidic channel.

could be removed in ethyl acetate; the soft microlens was thus successfully prepared. Taking advantage of the 3D fabrication capability, designability, and nanoscale accuracy, arbitrary 3D microlens profiles could be achieved using this FsLDW technique, which is almost impossible by any other microfabrication technologies. The strong capability of the FsLDW technique also allows fabrication of microlenses with different surface profiles, different sizes, and onto various substrates, revealing great potential for post-integration with given devices.

As typical examples, Fig. 1b–g shows a spherical microlens and an aspheric hyperboloid microlens viewed from different angles. It is noteworthy that the surface profile of our hyperboloid microlens is not a portion of a sphere. In fact, the profiles of a hyperboloid microlens could be defined as the following equation:

$$\frac{y^2}{a^2} - \frac{x^2}{b^2} = 1$$

where a and b are variable parameters that define the profile of our hyperboloid microlenses. In our work, two pairs of parameters ($a_1 = 8.87$, $b_1 = 9.56$; $a_2 = 47.47$, $b_2 = 51.13$) were used for the fabrication of a small microlens and a large hyperboloid microlens, respectively. In the former case, the radius (r) and the height (h) are 8.5 μm and 3.0 μm, respectively, whereas in the latter case, r is 20.0 μm and h is 3.5 μm. Since the refractive index (n) of PDMS is 1.47,[35] the focal length (f) of the resultant microlenses in air could be directly calculated from the following equation:

$$f = \frac{r^2 - (n^2 - 1)h^2}{2(n-1)h}$$

It is well known that spherical aberration can be effectively eliminated using a hyperboloid microlens. So the optical performance such as imaging quality can be improved using such a hyperboloid microlens. However, the difficulties with respect to fabrication limit their broad applications; nevertheless, with the help of the FsLDW technique, the programmable fabrication makes it much easier to reach this end.

In addition to the flexible designability of the lens profile, the FsLDW technique also allows integration of the microlens with given microdevices. As proof-of-concept, we fabricated a hyperboloid microlens within a microfluidic channel which was prepared beforehand. Fig. 1h shows an SEM image of a hyperboloid PDMS microlens embedded in a microfluidic channel. Notably, the integration of microlenses with microfluidic devices may trigger potential applications such as light focusing,[36] *in situ* monitoring, fluorescence collection and optical imaging.[37,38]

To get further insight into the surface profile of the as-obtained microlenses, the topographies of a spherical microlens and a hyperboloid microlens were characterized by AFM. As shown in Fig. 2, the hyperboloid microlens is ~17 μm in diameter, and the height is ~3 μm. Notably, the surfaces of the two microlenses are very smooth; a local surface smoothness was measured to be ~7 nm. As we know, the surface profile and surface roughness of a microlens play a very important role in

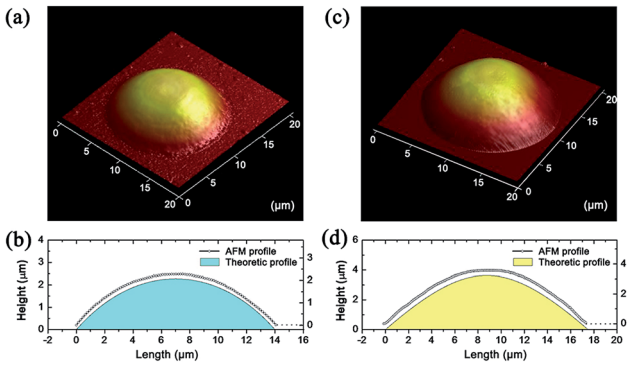

Fig. 2 (a) 3D AFM image of a spherical PDMS microlens. (b) The measured profile of the spherical PDMS microlens as compared with that of a theoretic model. (c) 3D AFM image of an aspheric hyperboloid microlens. (d) The measured profile of the aspheric hyperboloid PDMS microlens as compared with that of a theoretic model.

imaging performance. Poor smoothness would give rise to strong scattering and loss of light. Herein, a stable FsLDW system and optimized processing parameters (*e.g.*, scanning step, laser power and exposure duration) can allow the refined control of the surface smoothness; the high positioning accuracy due to the use of piezo moving stage with motion accuracy better than 1 nm or mirror steering with accuracy of several nanometers would ensure a highly precise surface profile. To make a clear-cut comparison between the profiles of as-obtained microlenses and their theoretic models, the profile curves of both spherical and hyperboloid PDMS lenses measured by AFM, as well as their theoretic profiles deduced from mathematic equations are shown in Fig. 2b and d. It can be clearly observed that, for both spherical and hyperboloid PDMS lenses, the measured profiles match well the theoretic values. The relative error of the two microlens profiles is very small, which would guarantee a very good optical performance.

The focusing capability of our PDMS microlens was investigated and characterized by optical microscopy. As shown in Fig. 3, a much larger PDMS hyperboloid microlens with a radius of ~20 μm, a height of ~3.5 μm, and a theoretical focal length of ~117 μm was used for the optical focusing tests (Fig. 3a). The white light focal spots of the PDMS hyperboloid microlens are quite sharp (Fig. 3b). Its measured focal length of ~112 μm in air is consistent with the theoretical value. Fig. 3b displays the normalized light intensity distribution along a line across the center of Fig. 3a. The full width at half maximum of the curve is ~8 μm, which indicates that the PDMS hyperboloid microlens has very good microlens efficiency. Fig. 3d shows a clear image of a Chinese word. Illustrations shown as insets of Fig. 3e exhibit the focal spots of PDMS hyperboloid microlens for monochromatic light of different wavelengths in air. Notably, the focal length increases with an increase of light wavelength; this could be attributed to the slight decrease of the refractive index of PDMS at longer wavelength. According to the focal equation of our microlens, a decrease of refractive index (n) would directly lead to the increase of focal length. In this

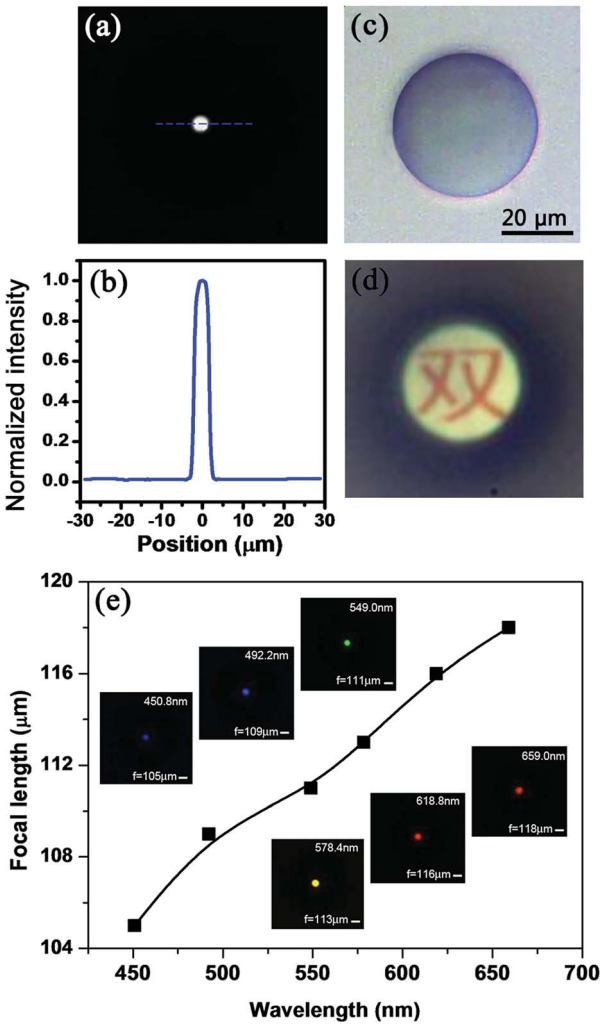

Fig. 3 (a) Focusing test of a hyperboloid PDMS microlens in air. (b) Normalized light intensity distribution along the blue dotted line in (a). (c) Optical microscopy image of a hyperbolic PDMS microlens. (d) Image of a Chinese word. (e) Focal spots of the hyperboloid PDMS microlens for monochromatic light of different wavelengths in air.

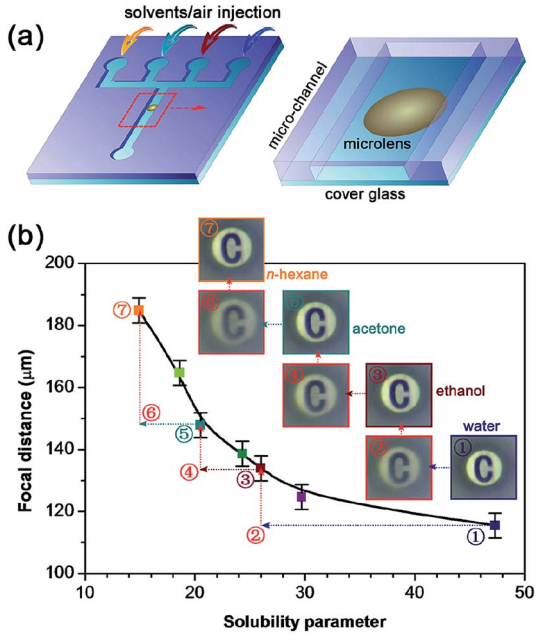

Fig. 4 (a) Schematic illustration of the integration of PDMS microlens with microfluidic device. (b) The dependence of focal length on the stimuli solvents of different solubility parameters. The insets are focused images of the PDMS microlens after the stimulation of different solvents.

experiment, the largest focal length shift was only ~7%, indicating a good optical performance.

It is well known that PDMS is very sensitive to organic solvents; most organic solvents would diffuse into the material and cause it to swell. Taking advantage of the swelling property of PDMS material, we found that our PDMS microlens exhibits solvent-responsive properties. Thus a solvent-tunable PDMS microlens has been proposed for the first time. Note that the swelling ratio is roughly inversely related to the solubility parameter of organic solvents. We design and fabricate a multi-channel microfluidic device, and a hyperboloid PDMS microlens has been integrated with the microchannels. Since the transformation between swelling and shrinking is due to the interaction of solvent and polymer network, dynamic tuning of the optical properties of our PDMS hyperboloid microlens using different organic solvents is viable. Fig. 4a shows a schematic illustration of the microfluidic device. A PDMS hyperboloid microlens with a radius of 20 μm and a height of 3.5 μm was integrated into a microfluidic channel with multiple channels for solvents/air injection and one channel for the solvents/air flowing out. The imaging feature of the PDMS hyperbolic microlens during the tuning process was characterized by optical microscopy. As shown in Fig. 4b, the focal length changes obviously under the stimulation of solvents. To avoid the influence of surrounding solvents on the focal length, an air segment was injected into the microchannel to expel the residual solvents in the channel for subsequent focal length measurements. In our experiments, we found that the focal length of the PDMS hyperboloid microlens increases when the solubility parameter of the stimuli solvents decreases from 47.3 to 14.9. Four kinds of solvents, namely water, ethanol, acetone and *n*-hexane with solubility parameters of 47.3, 26.0, 20.5 and 14.9, respectively, have been used for the focal length tuning. Note that the PDMS surface could not be wetted by water due to the hydrophobic property; thus after water stimulation, the focal length was measured to be 112 μm, which is the same as before. However, when ethanol was injected to stimulate the microlens, the focused image becomes blurry, indicating a change of focal length. Clear focused image could be restored when we increase the image distance, as shown in the insets of Fig. 4b. With a decrease of solubility parameter, here acetone and *n*-hexane were injected into the microfluidic channel, the focal length in air was measured to be 149 μm and 185 μm, respectively. According to the equation of our hyperbolic microlens shown above, the focal length in air is dominated by both the geometrical profile and refractive index of the material. Despite the swelling of the PDMS microlens in organic solvents slightly altering its refractive index (for water, ethanol, acetone,

n-hexane the refractive indexes are 1.33, 1.36, 1.36, 1.37, respectively), as compared with size change, this influence is negligible. The morphology changes were considered as the major reason for focal length changes. Based on the profile equation of our hyperbolic microlens, an increase of r or a decrease of h would lead to obvious increase of focal length. Considering the swelling behavior of PDMS in *n*-hexane, obvious increase in focal length might be attributed to the expansion in the radius. Despite the fact that the swelling of the microlens in organic solvents would slightly increase the surface roughness, a clear image could be also observed when we increase the image distance. Additionally, the response is reversible and the focal length could be tuned back when solvent was injected again. Additionally, since the microlens is very small, and the relatively large interface area would promote solvent diffusion, the response time is very short: fast swelling and shrinking could be accomplished within a few seconds. Taking advantage of the microfluidic technique, segment flow of different solvents and air could be easily switched. In this regard, the novel solvent-tunable microlens may impart promising functions to microfluidic devices.

To evaluate the tunable imaging performance of our PDMS microlens, a circle and a triangle were fabricated as target objects by FsLDW using SU-8 photoresist. As shown in Fig. 5, the two objects (circle and triangle) are placed at different distances. After water stimulation, the focal length of the PDMS microlens is not changed. A clear image of the triangle could be clearly observed by a microscope at the image plane. Very interestingly, without moving the two target objects and the image plane, a clear image of the circle could be observed after the stimulation of *n*-hexane, demonstrating the tunable imaging capability. The tunability could be attributed to an increase of focal length. According to our previous results, the focal length increased to ~185 μm after *n*-hexane stimulation, so the image of the triangle which is placed near the focal point is far away, whereas the image of the circle could be observed at the imaging plane. To get further insight into the swelling behavior, we observed the profiles of our microlens in both water and *n*-hexane. As shown in the insets of Fig. 5, an obvious increase in the diameter was observed after *n*-hexane stimulation, whereas the change of height was negligible. According to the focal length equation, the obvious increase of microlens radius would lead to an increase of focal length, in good agreement with our previous hypothesis. The origin of the anisotropic swelling could be attributed to the FsLDW technique, in which the microlens structure is fabricated by the overlapping of voxels. Since the voxel is ellipsoid-like in shape, the polymer network along the horizontal direction is much looser than that along the vertical direction, giving rise to the formation of an anisotropic polymer network.

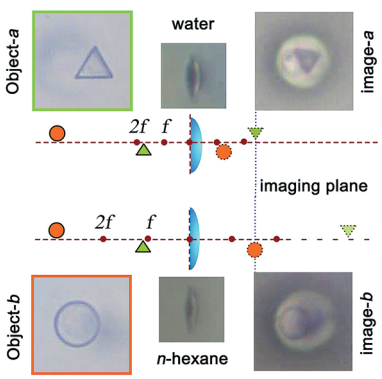

Fig. 5 Schematic illustration of the tunable imaging performance of the PDMS microlens after water and *n*-hexane stimulation. A circle and a triangle were fabricated as target objects, which were placed at different positions. The imaging plane was fixed at the right-hand side of the microlens. The insets are optical microscopic images of the objects, the microlens profiles, and the imaging of target objects.

Conclusion

In conclusion, PDMS microlenses with equation-defined profiles, such as spherical microlens and aspheric hyperboloid microlens, have been successfully fabricated by the FsLDW technique. The microlenses show smooth surface and very low relative error as compared with their theoretic values, which renders good imaging performance. Taking advantage of the "direct writing" feature, such microoptical components could be flexibly integrated with given microfluidic devices, which would bring new functionalities, such as light focusing, *in situ* monitoring, and optical imaging, to general microfluidic chips. Additionally, the focal length of the resultant PDMS microlenses could be dynamically tuned form 100% (previous value) to 160% when organic solvents of different solubility parameters were used as stimulators. The flexible fabrication and integration of solvent-tunable microlenses hold great promise for the development of novel functional microfluidic and optofluidic devices.

Acknowledgements

The authors would like to acknowledge the National Basic Research Program of China (grant number: 2011CB013000 and 2014CB921302), and NSFC (grant number: 61376123, 61435005 and 51335008) for support.

Notes and references

1 S. M. Kim, H. Kim and S. Kang, *Opt. Lett.*, 2006, **31**, 2710–2712.
2 C. Quan, S. H. Wang, C. J. Tay, I. Reading and Z. P. Fang, *Opt. Commun.*, 2003, **225**, 223–231.
3 S. Kuiper and B. H. W. Hendriks, *Appl. Phys. Lett.*, 2004, **85**, 1128–1130.
4 N. SoodBiswas, M. A. Sekh, S. Sarkar and A. Basuray, *Opt. Commun.*, 2012, **285**, 2607–2610.
5 Z. N. Tian, L. J. Wang, Q. D. Chen, T. Jiang, L. Qin, L. J. Wang and H. B. Sun, *Opt. Lett.*, 2013, **38**, 5414–5417.
6 R. P. J. Barretto, B. Messerschmidt and M. J. Schnitzer, *Nat. Methods*, 2009, **6**, 511–U561.

7 T. Mogi, K. Hatakeyama, T. Taguchi, H. Wake, T. Tanaami, M. Hosokawa, T. Tanaka and T. Matsunaga, *Biosens. Bioelectron.*, 2011, **26**, 1942–1946.

8 H. Wu, T. W. Odom and G. M. Whitesides, *Adv. Mater.*, 2002, **14**, 1213–1216.

9 W. L. Chang and P. K. Wei, *Opt. Express*, 2007, **15**, 6774–6783.

10 X. H. Yu, Z. Wang and Y. C. Han, *Microelectron. Eng.*, 2008, **85**, 1878–1881.

11 J. Y. Kim, K. Pfeiffer, A. Voigt, G. Gruetzner and J. Brugger, *J. Mater. Chem.*, 2012, **22**, 3053–3058.

12 S. M. Kim, H. Kim and S. Kang, *Opt. Lett.*, 2006, **31**, 2710–2712.

13 N. S. Ong, Y. H. Koh and Y. Q. Fu, *Microelectron. Eng.*, 2002, **60**, 365–379.

14 K. Sugioka and Y. Cheng, *Lab Chip*, 2012, **12**, 3576–3589.

15 Y. L. Zhang, Q. D. Chen, H. Xia and H. B. Sun, *Nano Today*, 2010, **5**, 435–448.

16 S. Kawata, H. B. Sun, T. Tanaka and K. Takada, *Nature*, 2001, **412**, 697–698.

17 S. H. Park, D. Y. Yang and K. S. Lee, *Laser Photonics Rev.*, 2009, **3**, 1–11.

18 Y. He, B. L. Huang, D. X. Lu, J. Zhao, B. B. Xu, R. Zhang, X. F. Lin, Q. D. Chen, J. Wang, Y. L. Zhang and H. B. Sun, *Lab Chip*, 2012, **12**, 3866–3869.

19 Y. Tian, Y. L. Zhang, J. F. Ku, Y. He, B. B. Xu, Q. D. Chen, H. Xia and H. B. Sun, *Lab Chip*, 2010, **10**, 2902–2905.

20 B. B. Xu, Y. L. Zhang, R. Zhang, L. Wang, X. Z. Xiao, H. Xia, Q. D. Chen and H. B. Sun, *J. Mater. Chem. C*, 2013, **1**, 4699–4704.

21 B. B. Xu, Y. L. Zhang, H. Xia, W. F. Dong, H. Ding and H. B. Sun, *Lab Chip*, 2013, **13**, 1677–1690.

22 B. B. Xu, R. Zhang, X. Q. Liu, H. Wang, Y. L. Zhang, H. B. Jiang, L. Wang, Z. C. Ma, J. F. Ku, F. S. Xiao and H. B. Sun, *Chem. Commun.*, 2012, **48**, 1680–1682.

23 S. Juodkazis, V. Mizeikis, S. Matsuo, K. Ueno and H. Misawa, *Bull. Chem. Soc. Jpn.*, 2008, **81**, 411–448.

24 T. W. Lim, Y. Son, Y. J. Jeong, D.-Y. Yang, H.-J. Kong, K.-S. Lee and D.-P. Kim, *Lab Chip*, 2011, **11**, 100.

25 D. Wu, Q. D. Chen, L. G. Niu, J. Jiao, H. Xia, J. F. Song and H. B. Sun, *IEEE Photonics Technol. Lett.*, 2009, **21**, 1535–1537.

26 D. Wu, S. Z. Wu, L. G. Niu, Q. D. Chen, R. Wang, J. F. Song, H. H. Fang and H. B. Sun, *Appl. Phys. Lett.*, 2010, **97**, 031109.

27 A. Žukauskas, K. K. Tikuisis, M. Sciuka, A. Melninkaitis, R. Gadonas, C. Reinhardt and M. Malinauskas, *Micro-optics*, 2012, **8428**, 84280K.

28 A. Werber and H. Zappe, *J. Microelectromech. Syst.*, 2008, **17**, 1218–1227.

29 Y. K. Fuh, M. X. Lin and S. Lee, *Optic. Laser. Eng.*, 2012, **50**, 1677–1682.

30 W. Zhang, H. Zappe and A. Seifert, *Light: Sci. Appl.*, 2014, **3**, e145.

31 L. Dong, A. K. Agarwal, D. J. Beebe and H. R. Jiang, *Nature*, 2006, **442**, 551–554.

32 Y. L. Sun, W. F. Dong, R. Z. Yang, X. Meng, L. Zhang, Q. D. Chen and H. B. Sun, *Angew. Chem., Int. Ed.*, 2012, **51**, 1558–1562.

33 C. A. Coenjarts and C. K. Ober, *Chem. Mater.*, 2004, **16**, 5556–5558.

34 J. L. Yong, F. Chen, Q. Yang, G. Q. Du, H. Bian, D. S. Zhang, J. H. Si, F. Yun and X. Hou, *ACS Appl. Mater. Interfaces*, 2013, **5**, 9382–9385.

35 P. Fei, Z. T. Chen, Y. F. Men, A. Li, Y. R. Shen and Y. Y. Huang, *Lab Chip*, 2012, **12**, 3700–3706.

36 L. Dong, A. K. Agarwal, D. J. Beebe and H. R. Jiang, *Nature*, 2006, **442**, 551–554.

37 P. Fei, Z. He, C. H. Zheng, T. Chen, Y. F. Men and Y. Y. Huang, *Lab Chip*, 2011, **11**, 2835–2841.

38 L. L. Qiao, F. He, C. Wang, Y. Cheng, K. Sugioka and K. Midorikawa, *Appl. Phys. A*, 2011, **102**, 179–183.